

# THE TUBE CHARACTER OF ELECTRON DRIFT IN CONDENSED INERT GASES

*E. B. Gordon*<sup>a\*</sup>, *B. M. Smirnov*<sup>b\*\*</sup>

<sup>a</sup>*Institute of Problems of Chemical Physics, Russian Academy of Sciences  
142432, Chernogolovka, Moscow Region, Russia*

<sup>b</sup>*Institute for High Temperatures, Russian Academy of Sciences  
127412, Moscow, Russia*

Submitted 11 February 2005

The behavior of an excess electron in condensed inert gases in an external electric field is considered at densities and temperatures at which the mobility of a slow electron is relatively high. On the basis of experimental data and a model of a pair electron interaction with atoms, an effective potential energy surface is constructed for an excess electron inside a dense inert gas. The region available for a slow electron consists of many intersecting channels that form a Delone network located between atoms. A drifting electron, as a quantum object, propagates along these channels (tubes), and electron transition between intersecting potential energy tubes of different directions provides an effective electron scattering. This mechanism of electron drift and scattering differs from that in gases and crystals. Peculiarities of electron drift inside dense inert gases are analyzed within the framework of this mechanism of electron scattering, leading to a moderate change of the electron mobility upon melting.

PACS: 34.80.-i, 52.80.Wq, 52.80.Yr, 79.20.Kz

## 1. INTRODUCTION

The reduced electron mobility of excess electrons in heavy condensed inert gases (Ar, Kr, Xe) as a function of the atom number density has a sharp maximum at moderate number densities, as it follows from experiments [1–14]. In particular, for xenon, the maximum zero-field reduced mobility exceeds that for a gaseous state by more than three orders of magnitude [6, 10]. Moreover, the maximum reduced zero-field mobility of excess electrons in inert gases exceeds that for coin metals by one order of magnitude [15].

The simplest theoretical models [16–20] consider the drift of an excess electron as a result of pair electron–atom scattering and explain high electron mobility by the Ramsauer effect in electron scattering on individual atoms and negative electron–atom scattering lengths for Ar, Kr, and Xe. But the approach of independent atoms is correct only for gases; at atomic densities corresponding to the maximum of the electron mobility,

the distance between nearest neighbors is comparable with the electron–atom scattering length, and hence this approach is not correct and may be considered rather as a model. The effect of high electron mobility at moderate atomic densities results from the collective character of the interaction of an excess electron with atoms.

Recently [21], we showed that the reason of the electron mobility maximum is related to the transition from attraction to repulsion for an excess electron inside an inert gas as the number density of atoms increases starting from the gaseous density. Indeed, in gases, where an excess electron interacts with each atom independently, the average electron potential energy is negative because of a negative electron–atom scattering length, which leads to an attractive Fermi exchange interaction of the electron with each atom. At high atomic densities, when the distance between neighboring atoms is comparable with the atom size, the average interaction potential for the electron corresponds to repulsion because of the Pauli exclusion principle. Hence, at moderate atom densities, the av-

---

\*E-mail: gordon@binp.ac.ru

\*\*E-mail: bsmirnov@orc.ru

erage interaction potential of an excess electron with inert gas atoms becomes zero.

Therefore, there is a range of inert gas densities with an attractive interaction potential for an excess electron, and these densities correspond to a high electron zero-field mobility, as is observed experimentally. Because penetration of an excess electron into each core leads to repulsion due to the Pauli principle, points of the maximum attractive potential for an excess electron form a Delone (Delaunay) network [22–24], whose lines are located between atoms and may be found on the basis of the Voronoi–Delone method [25]. This method consists in construction of planes located at identical distances from neighboring atoms. Intersections of these planes form the Delone network, and the electric potential has minima on this network. The equipotential surfaces that are close in energy form tubes, which are almost straight. The electron, being a quantum object, can propagate inside an inert gas along these almost straight channels. Electron transitions between channels of different directions in regions of their intersections lead to an effective electron scattering.

We thus conclude that a specific mechanism of the electron drift in this case differs from those in both gases and crystals. Indeed, propagating in gases, a test electron is scattered on individual atoms, whereas scattering of an electron wave in crystals is determined by distortion of the crystal lattice as a result of a shift of atom positions from the equilibrium ones during motion of the electron wave. Then melting of a solid should seemingly lead to a strong change of the electron mobility. However, in the case under consideration, a slow electron propagates along an individual tube near the Delone network, the electron scattering is weak, and therefore the electron mean free path inside an inert gas with optimal parameters is large compared to the distance between nearest neighbors. Correspondingly, change of the phase state does not lead to a significant change of the mobility for a slow electron in an inert gas.

Below, we consider the tube mechanism of electron drift in heavy inert gases and analyze various aspects of the electron drift under conditions of the tube-shape potential of a self-consistent field for an excess electron.

## 2. ELECTRIC POTENTIAL FOR AN EXCESS ELECTRON IN DENSE INERT GASES

The negative spatial charge created by excess electrons in dense inert gases can result in strong electric

fields even at low electron number densities. Therefore, we consider the regime of electron drift in an inert gas neglecting the interaction between individual electrons; that is, an individual electron is considered drifting in an inert gas. We consider peculiarities of the potential energy surface (PES) for an excess electron in an inert gas and, correspondingly, the character of the electron drift in condensed inert gases under the action of an external electric field. Using the analogy with clusters consisting of many atoms with a pair interaction between them [26–28], we represent the PES as a sum of local minima and saddles. At atomic densities, when the electron mobility is high, an excess electron passes over barriers of the PES during its drift in inert gases.

Another peculiarity of the PES at optimal atomic number densities is a large volume inside condensed inert gases where the electron location is prohibited by the Pauli exclusion principle. Indeed, a slow electron cannot penetrate inside an atom where valence atomic electrons are located, and hence the excluded region for an excess electron is concentrated near atomic cores. For simplicity, we take the prohibited volume near each atom in the form

$$V_* = \frac{4\pi}{3} r^3, \quad (1)$$

where  $r$  is the effective atom radius, which depends on the electron energy  $\varepsilon$ . We take it from the relation

$$U(2r) = \varepsilon,$$

where  $U(R)$  is the interaction potential of two atoms at a distance  $R$  between them. In this way, we changed the repulsion of a free electron from the atom core by that of a bound electron. Table 1 lists the values of the atom radii for an exchange electron–atom interaction calculated on the basis of the above formula. This volume is compared in Table 1 with the volumes per atom for the solid  $V_{sol}$  and liquid  $V_{liq}$  phase states at the triple point, and also with the volume per atom  $V_{max}$  at the atomic number density that corresponds to the maximum of the electron mobility. These ratios are given for the electron energy  $\varepsilon = 0.1$  eV and for the electron energy  $\varepsilon = 1$  eV in parentheses. We can see that the prohibited volume for a free electron at low electron energies may occupy a significant part of the total volume.

We note that this character of the exchange interaction between an excess electron and valence electrons of atoms of condensed inert gases is preserved up to high atomic densities until electron shells of neighboring atoms overlap significantly. In any case, it is valid at densities related to the solid and liquid aggregate

**Table 1.** Parameters of the repulsive interaction potential for an excess electron with individual atoms of inert gases

	Ar	Kr	Xe
$\bar{r}, a_0$	1.663	1.952	2.338
$\overline{r^2}, a_0^2$	3.311	4.455	6.277
$r, \text{Å}, \varepsilon = 0.1 \text{ eV}$	1.63	1.72	1.92
$r, \text{Å}, \varepsilon = 1 \text{ eV}$	1.23	1.28	1.30
$V_{sol}, \text{cm}^3/\text{mol}$	24.6	29.6	37.1
$V_{liq}, \text{cm}^3/\text{mol}$	28.2	34.3	42.7
$V_{max}, \text{cm}^3/\text{mol}$	50.2	43.0	50.2
$V_*/V_{sol}$	0.44(0.19)	0.44(0.18)	0.48(0.15)
$V_*/V_{liq}$	0.39(0.17)	0.38(0.15)	0.42(0.13)
$V_*/V_{max}$	0.22(0.10)	0.30(0.12)	0.35(0.11)

states of inert gases, and the average exchange interaction potential at a given atomic density due to this interaction can be approximated by the formula

$$U_{ex} = A \exp\left(-\alpha \frac{V_*}{V}\right), \quad (3)$$

where  $V$  is the volume per atom, and  $A$  and  $\alpha$  are parameters.

We now construct the difference between the potential for an excess electron located inside a condensed inert gas and in a vacuum. Taking the electron potential in a vacuum to be zero, we vary the atomic density from low values, when this system of atoms is a gas, up to moderate ones, at which the mobility of an excess electron is of interest. At low atomic densities, an excess electron interacts with individual atoms independently. In regions between atoms and far from them, the interaction potential is zero, and nonzero interaction takes place only near the atoms. On the basis of the Fermi formula [29, 30], the interaction potential between an electron and atoms can be represented as

$$U(\mathbf{r}) = \sum_i \frac{2\pi\hbar^2}{m_e} L\delta(\mathbf{r} - \mathbf{R}_i), \quad (4)$$

where  $\hbar$  is the Planck constant,  $m_e$  is the electron mass,  $\mathbf{r}$  is the electron coordinate,  $\mathbf{R}_i$  is the coordinate of the  $i$ th atom, and  $L$  is the electron–atom scattering length. Because the scattering length  $L$  is negative for Ar, Kr, and Xe (see Table 2), this interaction potential corresponds to attraction in the regions close to atoms. Therefore, the potential energy surface consists

**Table 2.** Parameters of the potential energy for an excess electron inside inert gases

	Ar	Kr	Xe
$L, a_0$	-1.5	-3.1	-5.7
$U_{min}, \text{eV} [8, 11, 12, 14]$	-0.33	-0.53	-0.77
$N_{min}, 10^{22} \text{ cm}^{-3}$	1.1	1.2	1.1
$a_{min}, \text{Å}$	4.8	4.7	4.8
$r_{min}, \text{Å}$	2.8	2.7	2.8
$2\pi\hbar^2 LN_{min}/m_e, \text{eV}$	0.41	0.94	1.58
$C, \text{eV}$	0.44	0.71	1.04
$\alpha$	4	4	4
$A, \text{eV}$	6	10	14
$R_{min}, \text{Å}$	3.6	3.5	3.6
$C', \text{eV}$	0.15	0.25	0.36
$A', \text{eV}$	2.2	3.5	6.5

of regions inside atoms with a sharp electron repulsion, regions near each atom with electron attraction, and regions between atoms with zero interaction potential. The attraction corresponds only to an average interaction of an electron of zero energy with an individual atom in a gas, and according to formula (4), the average interaction potential of an electron with inert gas

atoms is given by

$$\bar{U}_{at} = \frac{2\pi\hbar^2}{m_e}LN, \quad (5)$$

where  $N$  is the atom number density. This interaction leads to a red shift of spectral lines emitted by excited atoms located in inert gases [31]. Because this shift of spectral lines is determined mostly by the exchange electron–atom interaction, and a long-range interaction, including the polarization ion–atom interaction, gives a small contribution to this shift, we account below for the exchange part of the interaction only.

The exchange interaction of a test electron with electrons of an internal atom region corresponds to repulsion of this electron, and we describe it by formula (3). Adding the attractive exchange interaction potential (5) to it, we represent the total electron potential in the form

$$\bar{U}(N) = -C\frac{N}{N_{min}} + A \exp\left(-\alpha\frac{N_{min}}{N}\right), \quad (6)$$

where  $N$  is the current number density of atoms and  $N_{min}$  is the number density at which the interaction potential has a minimum. The values of  $N_{min}$  together with  $a_{min}$ , the distances between nearest neighboring atoms at this density, are given in Table 2.

If formula (6) is valid for a gas, where the second term is zero, the parameter  $C$  is equal to

$$C = -\frac{2\pi L\hbar^2}{m_e}N_{min}. \quad (7)$$

In reality, we are based on the experimental dependence  $\bar{U}(N)$  that gives another value of  $C$ . Indeed, on the basis of experimental data, which are approximated by formula (6), we find the parameters in Eq. (6) in accordance with the formula

$$C = -\frac{d\bar{U}}{dx}(x=0), \quad \alpha = \frac{C}{C - |U_{min}|}, \quad (8)$$

$$A = (C - |U_{min}|)e^\alpha, \quad x = N/N_{min}.$$

Here,  $U_{min}$  is the minimum of the electron potential inside an inert gas (the electron potential in a vacuum is zero). Experimental parameters for  $U(x)$  together with the parameters in formula (6) are given in Table 2. Figure 1 represents experimental data for the average electron potential energy in xenon.

Based on the experimental data for the electric potential of a condensed inert gas with respect to an excess electron, we construct the potential energy surface for an excess electron inside an inert gas. We rewrite

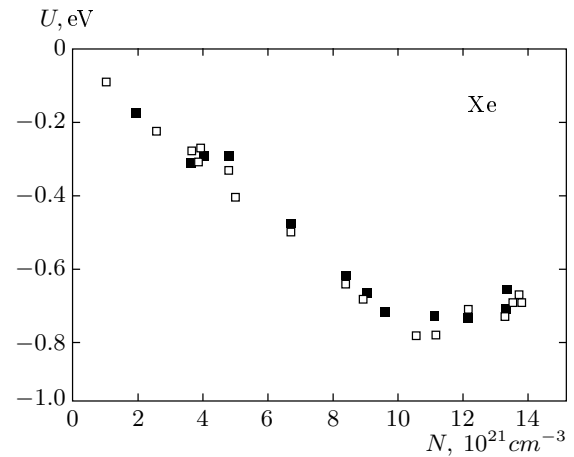


**Fig. 1.** The potential energy of an excess electron moving in xenon in an external electric field with respect to the vacuum vs the number density of atoms according to experiment [8] (symbols)

formula (6) for the minimal electron energy of an excess electron as

$$\bar{U}(r_W) = -C\left(\frac{r_{min}}{r_W}\right)^3 + A \exp\left(-\alpha\frac{r_W^3}{r_{min}^3}\right), \quad (9)$$

where

$$r_W = \left(\frac{4\pi N}{3}\right)^{-1/3}$$

is the Wigner–Seitz radius and  $r_{min}$  is the radius at the atom number density corresponding to the maximum attraction of an electron inside the inert gas. Formula (9) can be rewritten in terms of the distance  $a$  between the nearest neighbors,

$$\bar{U}(a) = -C\left(\frac{a_{min}}{a}\right)^3 + A \exp\left(-\alpha\frac{a^3}{a_{min}^3}\right), \quad (10)$$

where  $a_{min}$  is the distance between nearest neighbors at which the electron potential inside an inert gas has the minimum. We note that the atom number densities corresponding to the minimum of the electron potential according to formulas (9) and (10) are equal to  $N_{min}$ , the minimal electron potentials in formulas (9) and (10) coincide with  $U_{min}$ , and these parameters follow from formula (6). In addition, we assume a classical character of the electron interaction inside an inert gas in this consideration, although the interaction has a quantum character in reality.

### 3. DELONE NETWORK FOR THE INTERACTION OF AN EXCESS ELECTRON INSIDE AN INERT GAS

Our goal is to construct the potential energy surface for an excess electron inside an inert gas in the range of the atom number densities and temperatures providing an attractive electric potential there. We concentrate on the simplest case where atoms form a crystal lattice and find electron positions with the minimum potential energy. Evidently, because of the repulsive interaction for an excess electron with atom interiors, the points of the minimum electron potential are located equidistantly from the nearest nuclei. For two nearest planes of the crystal lattice, we then draw the Voronoi surfaces between each pair of nearest neighbors, such that these surfaces separate the action of individual atoms on an electron. Each Voronoi plane is located at identical distances from two nearest atoms, and intersections of the Voronoi surfaces with the two considered planes of atoms are shown in Fig. 2, where they form a net of regular hexagons whose centers are the nuclei of the lattice. Evidently, from the symmetry considerations, the optimal positions of an excess electron with minimal values of the electron potential energy are located in the plane in the middle between the nearest planes of atoms considered. Intersections of the Voronoi surface with this plane form straight lines of three directions, the solid lines in Fig. 2.

Evidently, the electron potential energy is minimal on these lines forming the Delone network [22–24]. We note that the Delone network is an important mathematical concept (see, e.g., [32–34]). We here use only the applied aspect of this problem related to the construction of lines of the minimum or maximum potential (see, e.g., [25]). Electron drift inside an inert gas proceeds near these lines. We assume that intersection points of these lines, i.e., sites of the Delone network, are characterized by minima of the electron potential energy, and their values are identical for all the intersection points (values 4 in Fig. 2) because of the symmetry. Passing to three-dimensional space, we obtain intersections of six straight lines at points whose distance from two nearest neighbors is  $a/2$ , where  $a$  is the distance between nearest neighbors of the lattice.

Thus, assuming the optimal distance of an excess electron from nearest nuclei at the optimal number densities of atoms to be maximum for the minimum electron potential energy, we obtain the optimal electron positions for the close-packed crystal lattice to be located on the Delone network that consists of intersecting straight lines. We have two types of these

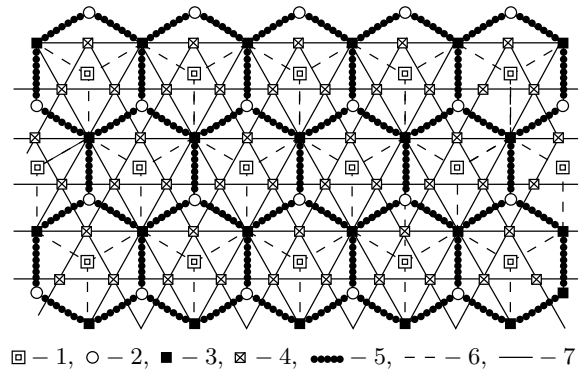


**Fig. 2.** The character of the behavior of an excess electron between two planes of the crystal lattice of inert gases: 1 — positions of atoms of the first layer, 2 — positions of atoms of the second layer, 3 — vertices of the pentagons that are intersections of the Voronoi surface with the corresponding layer, 4 — positions of the Voronoi surface for an excess electron in the middle plane between these layers with the strongest interaction between the electron and atoms, 5, 6 — hexagons that are intersections of the Voronoi surface with the corresponding layers, 7 — directions of the electron current if it is located in the middle plane

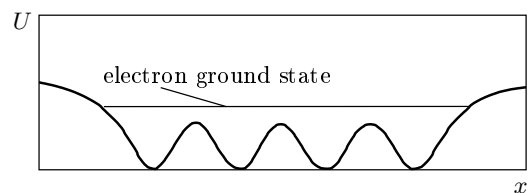


**Fig. 3.** The form of the potential energy for an excess slow electron in a condensed inert gas along lines of the Delone network

lines, which are alternated, and the period of translation symmetry is  $a$  for the first-type lines and  $a/2$  for the second-type lines. In Table 3, we give the distances from six nearest neighbors for points that correspond to the minima of the electron potential energy or are located in the middle between nearest such points. The number of nuclei with an indicated distance from a given point of the Delone network is given in parentheses.

In the liquid aggregate state, the Voronoi surfaces and Delone network may be constructed in the same manner, but the Delone network lines become curved. Nevertheless, because of a short order in liquids, the curvature of these lines is not large, and we can take the crystal case as a basis for a qualitative consideration.

**Table 3.** Distances between an excess electron located in minima and maxima of the Delone network and six nearest nuclei in the case where atoms form a close-packed crystal lattice. A number of nearest neighbors at an indicated distance is given in parentheses

	Points 4 in Fig. 2	In the middle between points 4 in Fig. 2
Lines of the first type	$\frac{a}{2}(2), a\frac{\sqrt{3}}{2}(4)$	$\frac{a}{\sqrt{2}}(6)$
Lines of the second type	$\frac{a}{2}(2), a\frac{\sqrt{3}}{2}(4)$	$\frac{a\sqrt{3}}{4}(1), a\frac{\sqrt{7}}{4}(2), a\frac{\sqrt{11}}{4}(1), a\frac{\sqrt{15}}{4}(2)$

In any case, the number of lines and the character of their intersection is identical in both cases. Supposing that positions on the Delone network correspond to the minimal electron potential inside an inert gas, we obtain that slow electron drifts inside the condensed inert gas near the lines form the Delone network. If we move along a given line of the Delone network, the electron potential energy oscillates, as is shown in Fig. 3. The behavior of the electron PES on the Delone network lines and near them resembles that for bound atoms in clusters [26–28], with the potential energy surface including many potential wells separated by barriers or saddles. But based on the experimental data for electron mobility, we take the difference between neighboring minima and maxima of the potential energy to be relatively small if the atom number density is near that corresponding to the maximum electron mobility [21].

#### 4. POTENTIAL ENERGY SURFACE FOR AN EXCESS ELECTRON INSIDE INERT GASES

We have found the character of distribution of the electron potential inside condensed inert gases in the density range where the electron potential energy is negative and close to the minimal one. The lines of a significant electron attraction inside an inert gas form a Delone network, and this result is not based on the assumption of a pairwise character of the electron–atom interaction. We use this assumption at the next stage of evaluation of the electron PES near the lines of maximum attraction, representing the interaction potential of an electron with surrounding atoms in the form of pair interaction potentials  $u(r)$  of this electron with nearest atoms,

$$U = \sum_i u(r_i), \quad (11)$$

where  $r_i$  is the distance of the electron from the  $i$ th nucleus and the pair interaction potential is taken such

that formulas (6) and (9) give the minimal electron energy inside an inert gas. Because of a short-range character of the electron interaction, we account for only six nearest neighbors. We take the dependence  $u(r)$  to be identical to that given by formula (10),

$$u(r) = -C' \left( \frac{R_{min}}{r} \right)^3 + A' \exp \left( -\alpha \frac{r^3}{R_{min}^3} \right). \quad (12)$$

This interaction potential has the minimum at the distance  $R_{min}$ .

Within the framework of this model, we represent the observed electron potential inside an inert gas as the average for points 3 and 4 in Fig. 2. Then on the basis of the data in Table 3, we have that the observed electron potential energy  $\bar{U}(N)$  at a given number density  $N$  of atoms is

$$\bar{U}(a) = u\left(\frac{a}{2}\right) + 2u\left(a\frac{\sqrt{3}}{2}\right) + 3u\left(\frac{a}{\sqrt{2}}\right). \quad (13)$$

Taking this relation at the minimum of the electron potential, i.e., at  $a = a_{min}$ , and expanding the interaction potential  $u(r)$  near its minimum,

$$u(r) = u(R_{min}) + \frac{u''(R_{min})}{2}(r - R_{min})^2,$$

we obtain the minimal electron potential

$$\begin{aligned} \bar{U}(a_{min}) &= u\left(\frac{a_{min}}{2}\right) + 2u\left(a_{min}\frac{\sqrt{3}}{2}\right) + \\ &+ 3u\left(\frac{a_{min}}{\sqrt{2}}\right) = 6u(R_{min} \pm \Delta R), \end{aligned} \quad (14)$$

where

$$\begin{aligned} R_{min} &= \frac{1 + 2\sqrt{3} + 3/\sqrt{2}}{12} a_{min} = 0.726a, \\ \Delta R &= \pm 0.123a_{min}, \quad \frac{\Delta R}{R_{min}} = \pm 0.17. \end{aligned} \quad (15)$$

The above estimates together with relation (13) allow us to determine the parameters of the interaction potential  $u(r)$  taken in form (12); they are listed in Table 2.

This approach allows us to construct the potential energy surface of an excess electron inside inert gases based on experimental data. Although the model uses a pair interaction between an excess electron and inert gas atoms, this is not of importance at the final stage of the analysis, because parameters of this model are taken from experimental results. In other words, the general character of the electron interaction is based on the Delone network and does not include the pairwise character of the electron interaction inside an inert gas, whereas the values of the electron potential includes this assumption. Therefore, the above behavior of the electron PES is valid strictly, while the accuracy of the values of the electron potentials at a given electron position are valid qualitatively.

### 5. ELECTRON DRIFT AT OPTIMAL DENSITIES OF INERT GASES AND LOW ELECTRIC FIELDS

The above analysis allows us to schematically draw equipotential surfaces for an excess electron inside an inert gas at a given number density of atoms, when the mobility of a slow excess electron is high. The lines of the minimum potential energy then form a Delone network, and for the crystal state of an inert gas, these lines are straight and pass between nearest atoms. A general shape of lines of the minimum potential energy are also correct for liquids in principle. Indeed, first, a change of the number density of atoms resulting from the solid-liquid phase transition for inert gases is approximately 15 %, and a change of the average distance between atoms is correspondingly 3 times less. Second, the distortion of lines of the minimal potential for an excess electron is also inessential because a slow electron is a quantum object, and the difference of the electron potentials inside and outside an inert gas allows us to find the energy of the electron level inside the inert gas, but not the minimum potential for an excess electron inside it. Correspondingly, the de Broglie wavelength is not small for a slow excess electron and a weak distortion of straight lines of the minimum electric potential for an excess electron, in passing from a solid to a liquid, is not of importance. Hence, our consideration relates simultaneously to the solid and liquid states of condensed inert gases.

Thus, we consider motion of a slow electron inside an inert gas whose density corresponds to electron at-

traction inside it. Therefore, an electron is bound inside the inert gas and moves along tubes centered at lines of the minimum electron potential, which are represented in Fig. 2 for a solid inert gas. These tubes of identical potentials are widened slightly near their intersections, and the distances between neighboring points of tube intersections is  $a\sqrt{3}/2$ , as follows from Fig. 2. When a slow electron propagates along a tube (see Fig. 3), its scattering proceeds in nodes of tube intersections, and as a result of this scattering, it transfers to another tube. We take the probability  $\gamma$  for the electron scattering in an intersection node to be small, and then the mean free path  $\lambda$  of an electron during its propagation along a potential tube is relatively large,  $\lambda \sim a/\gamma$  ( $\gamma \ll 1$ ).

Electron scattering in the intersection regions of potential energy tubes is similar to electron scattering on atoms in a gas because the time of strong interaction for an excess electron that causes scattering is a small part of the total time in both cases. In addition, in both cases, the electron is scattered mainly elastically, and only a small part of the electron energy ( $\sim m/M$ ) is transferred to nuclear heating ( $m$  is the electron mass and  $M$  is the atom mass). Below, we therefore use formulas for the electron drift velocity  $w$  and its average velocity  $v$  assuming that the electron is scattered in a gas (see, e.g., [35–37]). For an electron moving in an external electric field of a strength  $E$ , we then have

$$w \approx \frac{eE\lambda}{mv}, \quad v \approx \sqrt{\frac{M}{m}}w, \quad (16)$$

which gives

$$w \approx \left[ \frac{eEa}{\gamma(v)\sqrt{mM}} \right]^{1/2}, \quad v \approx \left[ \frac{eEaM^{1/2}}{\gamma(v)m^{3/2}} \right]^{1/2}. \quad (17)$$

In these formulas, we take the average electron velocity to be large compared to the electron thermal velocity in the absence of an external electric field. If this electric field is weak and does not change the Maxwell velocity distribution for excess electrons, the zero-field electron mobility  $K$  is

$$K \approx \frac{ea}{v\gamma}. \quad (18)$$

In evaluating the parameters of the electron drift, if it proceeds according to the above scheme, we are based on experimental data. Table 4 contains the number densities of atoms  $N_{max}$  and temperatures  $T_{max}$  of liquid inert gases [13] that provide the maximum zero-field mobility of electrons, the corresponding distances  $a_{max}$  between nearest-neighbor atoms, and the thermal electron velocity

$$v_t = \sqrt{8T_{max}/\pi m}$$

**Table 4.** Parameters of the drift of an excess electron in liquid inert gases under optimal conditions and low electric field strengths

	Ar	Kr	Xe
$T_{max}$ , K	155	170	223
$v_t$ , $10^6$ cm/s	7.7	8.1	9.3
$N_{max}$ , $10^{22}$ cm $^{-3}$	1.2	1.4	1.2
$a_{max}$ , Å	4.9	4.7	4.9
$K_{max}$ , cm $^2$ /V·s	1800	4600	6000
$\gamma_{min}$	0.0062	0.0022	0.0015
$E_*$ , V/cm	16	4.5	3.2

under these conditions. Then the above formulas give the minimal probability  $\gamma_{min}$  of electron scattering, which is a typical probability for the transition to another current tube at a point of tube intersection, and a typical electric field strength  $E_*$  at which a change in the average electron velocity due to the electron drift in an electric field is comparable to the initial thermal velocity. Starting from these electric field strengths, the electron drift parameters depend on the electric field strength.

We note that this mechanism for the electron drift, with the electrons propagating along the tubes whose centers form a Delone network, is valid only for some range of inert gas parameters at which the electron is locked inside the inert gas in regions near the Delone network. This mechanism of the electron drift provides high mobility for slow electrons, which can be used for determination of the range of the inert gas parameters and electric field strength where this mechanism of the electron drift applies. For xenon at least, these conditions are fulfilled in a wide range of the indicated parameters. An increase of the electric field strength leads to an increase of the electron energy and causes broadening of the region between atoms where an excess electron can be located. Finally, at high electron energies, the electron scattering changes from the tube character to scattering on atomic cores. Then the electron mobility decreases sharply with an increase of the electric field strength. In reality, for xenon, the experimental data analysis shows that this tendency exists, but the transition is not reached.

Electron scattering is also intensified if the gas parameters differ from the optimal ones. If the atom number density deviates from the optimal one, the attrac-

tive electron potential energy on the Delone network decreases, which leads to a stronger electron scattering in regions of tube intersection. At a given atom number density, the lower gas temperature, the higher is the electron drift velocity. This is explained by distortions in the atom distributions that increase as the temperature increases.

Thus, we represent the character of the drift of a slow electron in condensed inert gases under the optimal number density and temperature. The electron scattering under these conditions differs in principle from that in gases, where electrons collide with individual atoms separately. In this case, an electron is moving along a certain tube and transfers to another tube at points of their intersections. Axes of these tubes form the Delone network. This character of electron scattering also differs from the wave character of scattering in a crystal lattice, where scattering is determined by deviation of atom positions from the crystal lattice sites, such that scattering parameters vary significantly during the melting. In the case of the tube character of electron scattering, melting does not significantly change the electron drift parameters. We add that the tube character of the electron drift is realized in a restricted range of the inert gas parameters and is valid at not too high electric field strengths.

On the basis of this analysis, we can single out the range of parameters that corresponds to the maximum electron mobility in condensed inert gases. As the number density of atoms increases, the effective interaction for an excess electron with atoms of a condensed inert gas varies from attraction due to the exchange interaction with an individual atom because of a negative electron-atom scattering length to repulsion owing to the Pauli exclusion principle when the electron penetrates inside an atom. Evidently, the maximum electron mobility corresponds to moderate atomic number densities corresponding to the transition from the first form of interaction to the second one. Then the PES part of location of an excess electron consists of narrow tubes with intersections, and the electron can propagate along these tubes. As the number density of atoms increases, these tubes are destroyed in regions near atoms where the electron is locked. If the atomic number density decreases, tubes widen, and the electron may transfer more effectively to tubes of another direction. In both cases, the electron mobility decreases.

We note that a temperature increase leads to an increase of fluctuations in positions of individual atoms, which causes the destruction of a PES tube. But a pressure increase leads to a decrease of these fluctuations

and hence stabilizes the PES tube when the tube corresponds to optimal conditions. In analyzing the optimal conditions for the electron mobility, we are mostly based on experimental data. But experimental data of this problem study are fragmentary. Additional experimental studies are required in order to construct the optimal range in coordinates of the atomic number density, temperature, and electric field strength for each heavy inert gas (Ar, Kr, and Xe). We also expect from the subsequent experimental study that at high pressure, the electron mobility will decrease with an increasing pressure.

We also note the peculiarities of inelastic electron scattering in condensed inert gases. If the electron energy is not small, and the electron can be considered as a classical object, its inelastic scattering inside an inert gas is related to excitation of phonons, and each act of elastic scattering is accompanied by a loss of approximately the  $m/M$  portion of the electron energy; in other words, the process of inelastic scattering of a classical electron in a condensed inert gas is similar to that in rare gases. This is used in formulas (16) and (17). But a slow electron is a quantum object, and its inelastic scattering proceeds in another manner. Indeed, the electron states are characterized by discrete levels, and inelastic electron scattering requires its transition to an excited electron level. Therefore, at low electric field strengths, the inelastic electron scattering is weak and becomes the same as in a gas when the electron is excited sufficiently strongly, such that its levels are located sufficiently close.

In considering inelastic electron scattering, we restrict ourselves to just this limiting case. At high electric field strengths, the electron energy acquired from the field suffices for excitation of inert gas atoms. The excitation processes are in principle the same as in a gas, which are analyzed in detail in [37]. The efficiency of this process, that is, the electron energy part consumed to atom excitation, increases with an increase of the average electron energy  $\bar{\varepsilon}$  [15, 21] and is of the order of ten percent when the ratio  $\bar{\varepsilon}/\Delta\varepsilon \gtrsim 0.1$  ( $\Delta\varepsilon$  is the atom excitation energy). We are also guided by the experimental efficiency value of 18% in solid xenon [38, 39].

## 6. PECULIARITIES OF SELF-SUSTAINING DISCHARGE IN CONDENSED INERT GASES

An applied aspect of the phenomenon of electron drift in condensed inert gases is realized in electric dis-

charge, with the electric energy being converted into the energy of emitted photons in the vacuum ultraviolet spectrum range. Excess electrons drifting in condensed inert gases excite inert gas atoms, which leads to transformation of the electric energy into the energy of emitted photons. Because the electron energy is high, the efficiency of energy transformation is relatively high. During these processes, an excess electron cannot ionize the medium because its energy is below the ionization potential due to an effective atom excitation. The electrons are therefore injected into a sample from outside and only play the role of carriers of a negative charge, in contrast to standard gaseous discharges with ionization inside a sample. Due to this character of discharge maintenance, excess electrons create a non-compensated negative charge in condensed inert gases. This charge restricts the number density of excess electrons and correspondingly the power of the discharge and the intensity of yield radiation [42]. We find the maximum value  $N_e^{max}$  for the electron number density from the Poisson equation that has the form

$$\frac{dE}{dx} = -4\pi e N_e. \quad (19)$$

Here,  $E$  is the electric field strength,  $e$  is the electron charge,  $N_e$  is the electron number density, which is constant inside the inert gas layer, and the coordinate  $x$  is perpendicular to the inert gas layer whose thickness is  $l$ . From the Poisson equation, requiring  $E = 0$  in the layer middle because of the problem symmetry, we obtain the electric voltage  $U$  between the layer boundaries due to excess electrons inside the layer as

$$U = \pi e N_e l^2. \quad (20)$$

Formula (20) implies that the electron number density is the greater, the higher is the electric field voltage and the smaller is the layer thickness. In particular, under typical parameters  $U = 1$  keV and  $l = 1$  mm realized in experiments [38, 39], this formula gives  $N_e^{max} = 2 \cdot 10^{11}$  cm<sup>-3</sup>. This electron number density locks the electric current in discharge. We note that the number density  $N_e = 1 \cdot 10^{11}$  cm<sup>-3</sup> leads to the electric current density  $j \approx 0.01$  A/cm<sup>2</sup> and the discharge power  $P = Uj \approx 10$  W/cm<sup>2</sup>.

## 7. CONCLUSIONS

High electron mobility is observed in heavy condensed inert gases (Ar, Kr, Xe) in a narrow range of atomic densities. A widespread explanation of this effect [16–20] by the Ramsauer effect in electron scattering on an individual atom is not correct because of a

large distance of the electron–atom scattering in comparison with the distance between neighboring atoms at these atomic densities. In reality, the nature of high electron mobility is related to the transition from an attractive interaction potential between an excess electron and the atom ensemble to a repulsive one [21]. In this paper, we have proposed a new mechanism of electron drift in some range of atomic densities and temperatures near the optimal ones that provide the maximum electron mobility. This mechanism is additional to the character of electron drift in gases due to electron scattering on individual atoms and to electron drift in crystals due to scattering of the electron wave on nonuniformities of the crystal lattice.

This character of electron drift consists in propagation of an electron along almost straight channels; electron scattering occurs as a result of the electron transition to a propagation channel of another direction. This new mechanism of electron drift follows from the structure of the potential energy surface near its minimum; it consists of almost straight intersecting tubes, and the minimum of potential energy surface forms a Delone network. The tube character of the electron drift leads to high electron mobility. The understanding of this phenomenon allows us to choose optimal conditions for a self-sustaining electric discharge in condensed inert gases as a generator of ultraviolet radiation [38–40] and stimulates new experimental investigations.

This work is supported in part by the RFBR (grants №№ 04-03-32684, LSS-1953.2003.2).

## REFERENCES

1. H. Schnyders, S. A. Rice, and L. Meyer, *Phys. Rev.* **150**, 127 (1966).
2. L. S. Mi, S. Howe, and W. Spear, *Phys. Rev.* **166**, 871 (1968).
3. J. A. Jahnke, L. Meyer, and S. A. Rice, *Phys. Rev. A* **3**, 734 (1971).
4. T. Kimura and G. R. Freeman, *Can. J. Phys.* **52**, 2220 (1974).
5. K. Yoshino, U. Sowada, and W. F. Schmidt, *Phys. Rev. A* **14**, 438 (1976).
6. S. S.-S. Huang and G. R. Freeman, *J. Chem. Phys.* **68**, 1355 (1978).
7. S. S.-S. Huang and G. R. Freeman, *Phys. Rev. A* **24**, 714 (1981).
8. R. Reiniger, U. Asaf, and I. T. Steinberg, *Chem. Phys. Lett.* **90**, 287 (1982).
9. E. M. Gushchin, A. A. Kruglov, and I. M. Obodovskii, *Zh. Eksp. Teor. Fiz.* **82**, 1114 (1982).
10. V. V. Dmitrienko, A. S. Romanuk, S. I. Suchkov, and Z. M. Uteshev, *Zh. Tekh. Fiz.* **53**, 2343 (1983).
11. R. Reiniger, U. Asaf, and I. T. Steinberg, *Phys. Rev. B* **28**, 3193 (1983).
12. R. Reiniger et al., *Phys. Rev. B* **28**, 4426 (1983).
13. F. M. Jacobsen, N. Gee, and G. B. Freeman, *Phys. Rev. A* **34**, 2329 (1986).
14. A. K. Al-Omari, K. N. Altmann, and R. Reiniger, *J. Chem. Phys.* **105**, 1305 (1996).
15. B. M. Smirnov, *Usp. Fiz. Nauk* **172**, 1411 (2002).
16. J. Lekner, *Phys. Rev.* **158**, 130 (1967).
17. M. H. Cohen and J. Lekner, *Phys. Rev.* **158**, 305 (1967).
18. B. E. Springett, J. Jortner, and M. H. Cohen, *J. Chem. Phys.* **48**, 2720 (1968).
19. V. M. Atrazhev and I. T. Iakubov, *J. Phys. C* **14**, 5139 (1981).
20. V. M. Atrazhev and E. G. Dmitriev, *J. Phys. C* **18**, 1205 (1985).
21. E. B. Gordon and B. M. Smirnov, *Zh. Eksp. Teor. Fiz.* **125**, 1058 (2004).
22. B. N. Delaunay, in *Proc. Int. Math. Congr.*, Toronto (1924), Univ. of Toronto Press, Toronto (1928), p. 695.
23. B. N. Delaunay, *Z. Kristallogr.* **84**, 109 (1933).
24. B. N. Delone, *Usp. Math. Nauk* № 3, 16 (1937).
25. N. N. Medvedev, *Method of Voronoi–Delone in Study of Structure of Noncrystal Systems*, RAN SO, Novosibirsk (2000).
26. R. S. Berry, in *Theory of Atomic and Molecular Clusters*, ed. by J. Jellinek, Springer, Berlin (1999).
27. D. J. Wales, *Adv. Chem. Phys.* **115**, 1 (2000).
28. D. J. Wales, *Energy Landscapes*, Cambridge Univ. Press, Cambridge (2003).
29. E. Fermi, *Nuovo Chim.* **11**, 157 (1934).
30. M. Ya. Ovchinnikova, *Zh. Exp. Teor. Fiz.* **49**, 275 (1965).

31. H. S. W. Massey, E. H. S. Burhop, and H. B. Gilbody, *Electronic and Ionic Impact Phenomena*, 2nd. ed., Clarendon Press, Oxford (1969).
32. R. V. Galiulin, *Kristallogr.* **25**, 901 (1980).
33. R. V. Galiulin, *Kristallogr.* **43**, 366 (1998).
34. R. V. Galiulin, *Zh. Vychisl. Mat. Mat. Fiz.* **43**, 791 (2003).
35. L. G. H. Huxley and R. W. Crompton, *The Diffusion and Drift of Electrons in Gases*, Wiley, New York (1974).
36. B. M. Smirnov, *Physics of a Weakly Ionized Gases*, Nauka, Moscow (1978); Mir, Moscow (1981).
37. B. M. Smirnov, *Physics of Ionized Gases*, Wiley, New York (2001).
38. E. B. Gordon, G. Frossati, and A. Usenko, *Zh. Exp. Theor. Fiz.* **123**, 846 (2003).
39. A. Usenko, G. Frossati, and E. B. Gordon, *Phys. Rev. Lett.* **90**, 153201 (2003).
40. A. S. Schussler et al., *Appl. Phys. Lett.* **77**, 2786 (2000).
41. E. B. Gordon and A. F. Shestakov, *Low Temp. Phys.* **27**, 883 (2001).
42. E. B. Gordon, O. S. Rzhevskii, and V. V. Khmelenko, *Quant. Electr.* **21**, 209 (1994).
43. E. B. Gordon, V. V. Khmelenko, and O. S. Rzhevskii, *Chem. Phys. Lett.* **217**, 605 (1994).
44. B. M. Smirnov, *Usp. Fiz. Nauk* **171**, 1291 (2001).
45. V. M. Atrazhev, I. V. Chernysheva, and T. D. Doke, *Jpn. J. Appl. Phys.* **41**, 1572 (2002).